Discover Nano

Research

Bismuth sensitized iron oxide on exfoliated graphene oxide (Bi–Fe_2O_3@GO) for oxygen evaluation reaction

Akhtar Munir[1] · Shaheer Jamal[2] · Humaira Yasmeen Gondal[3] · Javed Iqbal[4] · Aamir Hussain[2] · Arslan Aziz[1] · Mahammad Nisar[3] · Muhammad Zubair[5] · Abdul Momin[6] · Ali Haider[1]

Received: 24 June 2024 / Accepted: 4 November 2024
Published online: 23 November 2024

Abstract
Electrochemical water splitting is a promising approach towards a sustainable and renewable energy source. However, the demand for high anodic potential and sluggish kinetics of oxygen evolution reaction (OER) restrict the efficiency and feasibility of the water-splitting process. In this quest, transition metal oxides and alloys are considered potential candidates owing to their natural occurrence and high redox potential for OER. However, many associated challenges in their use are still there to be addressed. Here, we designed a new class of bismuth-doped iron oxide on exfoliated graphene oxide by optimizing the metal loading on the conductive support to facilitate the flow of charge during catalysis. The catalytic ability of the synthesized Bi-doped nanocomposites was evaluated in activating the OER under extreme alkaline conditions (1 MKOH). On screening different combinations, 20Bi–Fe_2O_3@GO was identified as the most efficient and sustainable electrocatalyst even under harsh operating conditions, with an onset potential of 1.48 V and a Tafel slope of 65 mV/dec. The current study offers a new class of Bi-doped electrocatalysts, where the precise doping of Bi and the optimized loading of metal was found the key to achieving low onset potential and high current density to initiate OER.

Keywords Graphene nanocomposites · Bi–Fe_2O_3@GO · Electrocatalyst · Oxygen evolution reaction (OER) · Water-splitting

1 Introduction

Our environment is highly impacted by the overuse of unnecessary and exhaustible fossil fuels, which produce significant amounts of carbon dioxide. The need for renewable alternatives to address these crucial energy and environmental challenges is growing globally [1]. Water is an attractive choice to employ as a green, sustainable, and renewable source, where the need for the high anodic potential for the half-cell oxygen evolution reaction (OER) restrains the efficiency of the water-splitting process.Among different metal oxides, RuO_2 and IrO_2 are more efficient electrode materials to catalyze

Supplementary Information The online version contains supplementary material available at https://doi.org/10.1186/s11671-024-04146-x.

✉ Akhtar Munir, akhtarmunir991@gmail.com; akhtarmunir@qau.edu.pk; ✉ Humaira Yasmeen Gondal, hygondal@gmail.com; ✉ Ali Haider, ahaider@qau.edu.pk | [1]Present Address: Department of Chemistry, Quaid-i-Azam University, Islamabad, Islamabad 45320, Pakistan. [2]Department of Chemistry, University of Sialkot, Sialkot 51040, Pakistan. [3]Institute of Chemistry, University of Sargodha, Sargodha 40100, Pakistan. [4]Department of Botany, Faculty of Sciences, Bacha Khan University, Charsadda, Khyber Pakhtunkhwa, Pakistan. [5]Department of Physics, Sungkyunkwan University, University, 2066, Seobu-Ro, Jangan, Suwon, Gyeonggi-Do 16419, South Korea. [6]Department of Botany, Kohat University of Science and Technology, Kohat, Khyber Pakhtunkhwa 26000, Pakistan.

multi-step OER at low overpotential, but high cost and low availability restrict their applications on large [2]. Hence, developing efficient and cost-effective catalytic systems to reduce the substantial anodic bias for OER in the water-splitting process is highly desirable. The literature revealed that high Gibbs free energies of intermediates (M–OH, M–O, and MOOH) majorly contribute to initiating the OER process, where the "M–O" bonds with strong nucleophilic characteristics significantly restrict the attack of incoming nucleophiles (-OH) to control the chain reaction producing oxygen [3]. The optimal redox potential to catalyze OER depends on the active sites of metals, the nature of metal oxides, metal alloys, and metal hydroxides [4]. Ideal redox potential and abundant active sites of metal oxides and hydroxides are considered the best choice in catalyzing the OER process at the lowest overpotential. Moreover, nanohybrid metal alloys can further encourage their inherent redox properties [4], though poor conductivity and durability are their drawbacks [1]. The nanostructuring of metal oxides can be a promising alternative by tuning their electrocatalytic activity, selectivity, sustainability, and active site exposure [5]. The most important feature in developing nanocatalysis is the requirement of uniform dispersion of ultra-small and chemically stable nanomaterials on highly conducting surfaces, such as carbon nanotubes or graphene. Therefore, metal oxide and graphene-based nanohybrids can be promising options by fine-tuning electrical and catalytic properties as highly effective materials. Moreover, chemical exfoliation and functionalization such as doping of hetero atoms can improve the physicochemical and electronic properties of graphene-supported catalysts [6, 7]. Recently, Thomas et al. reported the incorporation of Bi into Cobalt borate and observed that OER performance is highly dependent on the optimum doping of Bi and consequent structural modification of metal borate [8]. Similarly, Anand et al. [9] reported the doping of alkaline earth metal (Ca) to Bi-ferrite to tune the electrochemical performance. However, a very high overpotential (2.12 V) was observed for OER [2].

Horn and his co-workers developed Bi-doped SrCo ($Bi_{0.2}Sr_{0.8}CoO_{3-\delta}$) for efficient OER with an onset potential of 1.55 V. It is deduced that the presence of Bi^{+3} acts as an acidic site and facilitate the adsorption of intermediate on the surface of Co during catalysis [4]. Very recently, Liqing Wu et al. [10] developed Bi-doped RuO_2 for OER in an acidic medium. It is found that the addition of Bii can increase the valance state of Ru to enhance the active site of Ru. Moreover, the doping of Bi can increase the structural stability by avoiding the overoxidation of Ru and hence perform long-lasting OER in an acidic medium [5] Above in view, the performance of such heterogeneous and multi-metal-based electrocatalysts especially transition metals can be further enhanced by changing the nature and concentration of doped metals and use of conducting support [11]**.** Therefore, we decide to explore Bi-composites for designing new, efficient, and cost-effective electrode materials for OER. In this perspective here we designed bismuth-doped iron oxide on the graphene oxide nanosheets as a sustainable low-cost electrocatalyst and different combinations of Bi–Fe_2O_3 and GO were screened to catalyze OER, where 20Bi–Fe_2O_3@GO was found the most efficient. Our encouraging results offer new possibilities in developing effective Bi-doped graphene-based nanohybrids to make water splitting a realistically viable method for sustainable energy.

2 Experimental section

2.1 Materials and reagents

Graphite powder (325 mesh, ≥ 80%, Alfa Acer), potassium permanganate ($KMNO_4$, ≥ 98%, Sigma Aldrich), potassium phosphate (H_3PO_4, ≥ 98%, Sigma-Aldrich), sulfuric acid (H_2SO_4, potassium hydroxide (KOH, ≥ 85%, Sigma-Aldrich), Bismuth nitrate ($Bi(NO_3)_3{\cdot}5H_2O$), Iron chloride ($FeCl_3.6H_2O$), diethyl ether ($(CH_3CH_2)_2$, ≥ 99%, Sigma-Aldrich), methanol, and ethanol (≥ 99.8%, Sigma-Aldrich) were used after double distillation.

2.2 Synthesis of graphene oxide

The Hummer method with some modifications [12, 13] was employed to synthesize graphene oxide (GO) by the reaction of graphite powder with potassium permanganate in the presence of sulfuric acid and sodium nitrate (Fig. 1). A typical procedure involves the stirring of a reaction mixture containing graphite powder (1 g), sodium nitrate (1 g), and H_2SO_4 (25 mL) at 0–4 °C. A slow addition of $KMnO_4$ (3 g), followed by dilution with distilled water (100 mL), was done to maintain the temperature. After 2 h, the temperature of the reaction mixture was gradually increased up to 35 °C and quenched with 30% H_2O_2 solution (50 mL). The recovered precipitates were centrifuged, washed several times with de-ionized water and 5% HCl solution, and oven-dried at 60 °C.

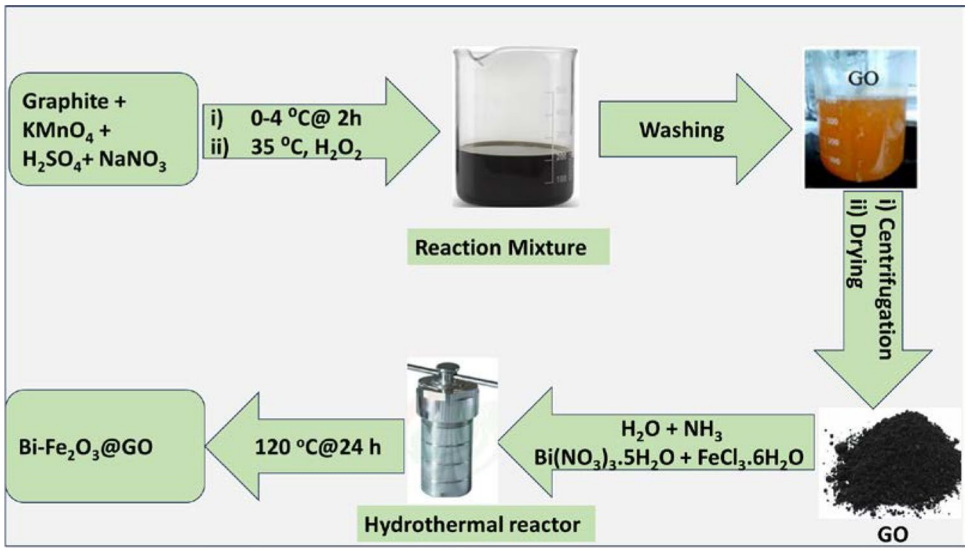

Fig. 1 Synthesis of Graphene Oxide (GO) by improved Hummer's method and loading of Bi–Fe_2O_3 by hydrothermal process

2.3 Synthesis of $BiFe_2O_3$@GO nanocomposites

Synthesis of the graphene oxide (GO) supported Bi-doped Fe_2O_3 was accomplished by employing a modified method (Fig. 1) [14]. For the 10% doping of Bi by mass with respect to Fe, a solution of $Bi(NO_3)_3{\cdot}5H_2O$ (0.3 mg) and $FeCl_3{\cdot}6H_2O$ (27 mg) in water (50 mL) was sonicated to ensure a homogenized mixing. The prepared graphene oxide (100 mg) dispersed in deionized water (100 mL) was added to the reaction mixture, and the pH (11–12) was maintained by adding liquid ammonia. The reaction mixture was stirred for 2 h at room temperature, and the recovered precipitates were washed with deionized water (200 mL). The obtained material was redispersed in water (50 mL), followed by 5 M NaOH solution (5 mL), and the reaction mixture was autoclaved at 120 °C for 24 h in a 100 mL stainless steel chamber with a Teflon liner. Finally, the solid material of $BiFe_2O_3$@GO was filtered, washed several times with ethanol, and dried under vacuum at 60 °C. The same procedure was adopted for the synthesis of different composites by using 20 and 30 percent of Bi for doping.

2.4 Characterization of $BiFe_2O_3$@GO nanocomposites

The synthesized materials were characterized by employing different techniques. A scanning electron microscope (NOVA FEISEM-450 was used to understand the morphology, while Energy dispersive X-rays (EDX, INCAX-Act equipped with a JASCO V66 detector were used to determine the impurities and composition. Transmission electron microscopy (TEM-JEM2100F, JEOL, 200 kV) was used for clear visualization of size and shape. Inductively coupled plasma optical emission spectroscopy (ICP-OES) was used for the determination of metal impurities before and after doping. In addition, X-ray diffraction (D2 Phaser, copper K-alpha) was used to evaluate the nature and phase purity of the material.

2.5 Electrochemical evaluation by $BiFe_2O_3$@GO nanocomposites

The electrochemical evaluation experiments were performed in an alkaline medium (1 M KOH) at room temperature using a potentiostat (Gamry 600) at 5 mA/cm^2. Glassy carbon (GC) was used as working electrodes, whereas platinum and Ag/AgCl wires were used as counter and reference electrodes. The working electrode was prepared by a simple drop-casting method, where a catalytic suspension (15 µL) was deposited and dried in air at ambient temperature. For preparing the suspension, the newly synthesized catalytic material (5 mg) was sonicated for 30 min in 0.5 mL of ethanol). The Linear Swap voltammetry (LSV) and chronopotentiometry (CP) measurements were performed in three electrode-setup experiments under alkaline conditions without *i*R correction to keep the originality of the data. The glass cell was properly washed (with dilute HCl) and dried before each experiment. Potential measuring data was taken against reversible hydrogen electrode (RHE) by using the standard Nernst equation:

$$E_{RHE} = E_{exp} + 0.0591*pH + E_{Ag/AgCl}$$

Tafel slope was determined in the potential range near the onset potential of the steady-state voltammogram [15]. Electrochemical impedance spectroscopy (EIS) was observed in the range of 0.1 Hz–1 MHz at a potential of 5 mV. LSVs were collected by preparing different percentages of the synthesized catalytic system (10 mg in 1 mL methanol) and nafion solution (5 µL) at a sonication of 30 min. The homogenous ink obtained was loaded on glassy carbon (GC) with an area of 0.07 cm^2 via the drop-casting method and allowed to dry at room temperature. LSVs were recorded in an anodic potential regime with a 5 mV/s scan rate. All the catalyst mixtures were scanned for ten cycles before collecting final data to ensure steady voltammograms.

3 Results and discussion

Electrocatalysts play a significant role in water splitting reactions, a crucial process in renewable energy systems, by reducing the energy requirement to facilitate the process. In search of new efficient, sustainable, and low-cost electrocatalysts here, we present a new graphene oxide (GO)-supported Bi-doped FeO_x electrocatalyst for the OER reaction. The amount of precursor and initiator was stoichiometrically optimized to control the Bi doping in the structure of iron oxide. Graphene oxide (GO) sheets are inherently highly conducting and possess various functionalities, such as aldehyde, ketone, carboxylic acid, and epoxides, to offer significant interactions with metal ions [16, 17]. Therefore, metal oxide nanoparticles can be successfully loaded on such a conducting support with uniform distribution.

3.1 Synthesis of graphene oxide (GO) supported Bi-doped Fe_2O_3 electrocatalyst

For synthesizing Bi-doped Fe_2O_3, the freshly prepared GO was ultrasonically dispersed in water to homogenize with the relevant metal salts. The homogeneous slurry was allowed to react under high pressure in an autoclave at 120 °C in an alkaline medium to facilitate the nucleation and growth of the metal NPs on graphene support (Bi–Fe_2O_3@ GO). Different percentages of loadings i.e., 10, 20, and 30 Bi–Fe_2O_3@GO have been synthesized and evaluated for OER to explore the role of doping in structural modification of cost-effective materials for electrocatalysis (Fig. 1).

3.2 Characterization of the $BiFe_2O_3$@GO nanocomposites

Compositional and structural characterization of the synthesized $BiFe_2O_3$@GO nanocomposites was accomplished by employing state-of-the-art techniques that include Scanning electron microscopy (SEM), energy dispersive X-ray spectroscopy (EDX), and X-ray diffraction (XRD) techniques. The size, shape, morphology of the nanocomposites, and the effect of Bi loading were analyzed by SEM [18]. Graphene oxide (GO) was observed in a refined shape with well-defined edges of sheets (Fig. 2)**.** Various oxygenated functionalities present on the surface of GO are considered responsible for developing interactions with metal to stabilize the synthesized nanocomposites. Figure 2a and b demonstrate a plane surface of graphene oxide sheets in the absence of NPs, while the small white spots on the surface represent the uniform loading of 20Bi–Fe_2O_3 on GO (Fig. 2c, d). A careful analysis of SEM images further revealed that Bi–Fe_2O_3 is encapsulated within the nanocomposites. The even distribution of metal nanocomposites on the support suggests the involvement of functionalities, which can enhance the trapping capability of the exfoliated graphene oxide and effectively prevent the agglomeration of Bi–Fe_2O_3. Moreover, the interface between metal-GO possibly plays a significant role in providing active sites for catalysis. However, increasing and decreasing the amount of doped Bi leads to agglomeration or loading of less amount of particles, respectively (Fig S1).

Further, the size, appearance, and distribution of particles were analyzed with TEM in comparison with bare GO as shown in Fig. 3. The TEM analysis further verified the extended sheet-like structure of GO which can facilitate the loading of materials at the nanoscale length Fig. 3a. The Fig. 3b–d shows the representative sample with 20%Bi doping at low and high resolution. It is observed that the surface of GO becomes black and loses transparency after loading of the particles. However, by magnifying the particles under TEM analysis, the edge of support can be seen uniformly covered by loading particles. TEM analysis further justifies that uniform distribution of particles can be achieved by controlling the stochiometric amount of metal precursors during synthesis.

The elemental composition of bared and metal-loaded nanocomposites (Bi–Fe_2O_3@GO) was analyzed by EDX [18]. Figure 4a shows the EDX spectrum of GO with the appearance of two peaks for C and O. The appearance of a peak for O suggested the presence of oxygen-containing functionalities on the surface of GO. Figure 4b-d shows the EDX spectrum

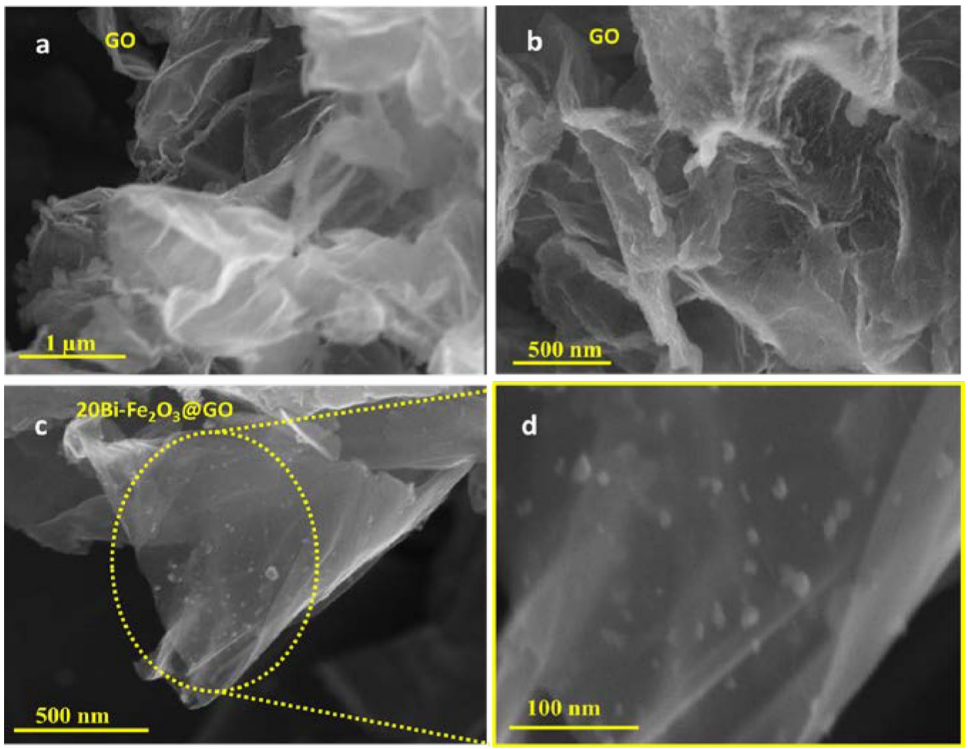

Fig. 2 SEM images of GO (*above*) and 20Bi–Fe_2O_3@GO (*below*) with low and high magnification

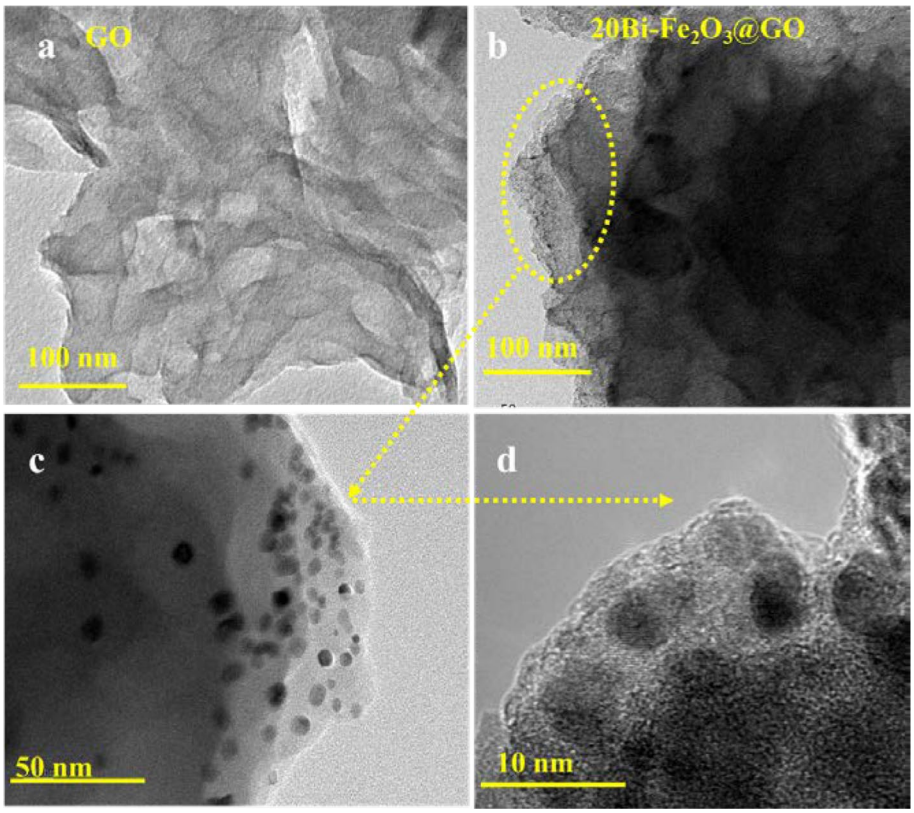

Fig. 3 **a** TEM images of GO and **b**–**d** 20Bi–Fe_2O_3@GO with low and high magnification

of different Bi–Fe_2O_3@GO, where the composite was coated with Au to enhance the conductivity and visualization under an electron beam. The oxygen content in all samples indicated atmospheric oxygen and partial surface oxidation of the graphene support. The appearance of Fe and Bi peaks confirmed the successful loading of Bi–Fe_2O_3 on the graphene

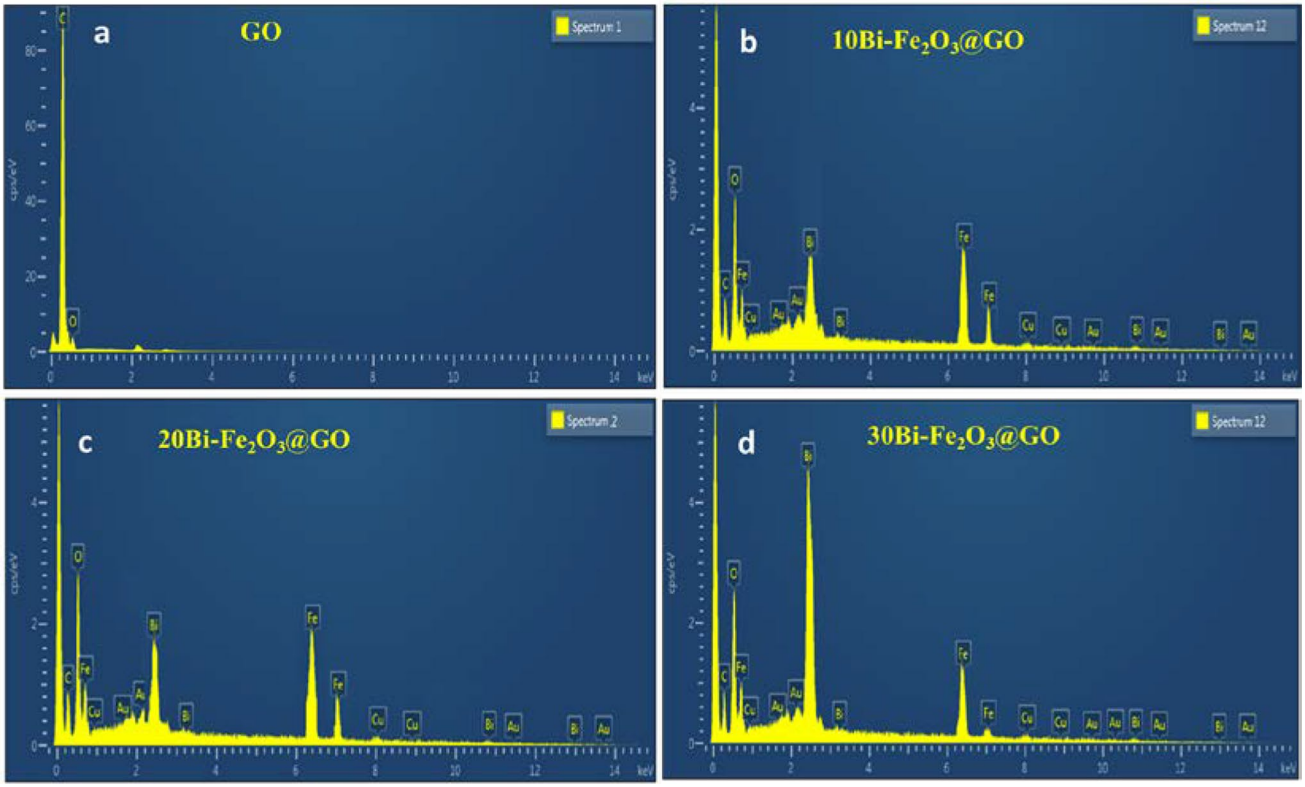

Fig. 4 EDX spectra of GO and all Bi–Fe_2O_3@GO with different Bi doping

surface in different compositions. By increasing the concentration of Bi, there is no change in the EDX spectra except a little bit of change in the intensity of the peaks which entails the effect of Bi loading. The presence of carbon is for graphene support, whereas an increase in the intensity of oxygen peaks suggests the possibility of FeO_x formation. The presence of Cu was due to the sample holder used during the analysis.

The metal content was further confirmed by ICP-OES with and without doping (Table S3). A minor difference in the theoretical and experimentally calculated metal contents was observed which is probably due to the interference phenomenon and the presence of the small amount of alkali and alkaline earth metals in water and acid used for the sample digestion. The X-ray diffraction study provides information about the crystal structure and phase purity of the materials [19]. The XRD pattern of pure GO shows the emergence of two peaks at 2θ = 10° and 27° due to the diffraction from (001) and (002) plan of GO, respectively (Fig S2a). The XRD pattern observed at 2θ = 22.2°, 28.5°, 30.2°, and 31.2° are raised from the crystal plane of Bi [20]. The peaks at 2θ = 37.5°, 46.2°, 53.8°, 57.3°, indicate the presence of Fe_2O_3 (JCPDS 33–0664) (Fig S2b). The loading of Bi-doped Fe_2O_3 on the surface of GO can be observed in Fig S2c which exactly matches with the peaks observed in Fig S2a, b. However, a minor shift in the peak of GO at $2\theta = 10^0$ may be due to the loading of Bi–Fe_2O_3. The Different intensities indicated different phases of a plane with different orientations (Fig S1b–c). Some other peaks of low intensities suggest that a minor quantity of Bi and Fe can be present in the different crystalline phases which is unclear and subject of future investigation [21].

3.3 Electrochemical evaluation

To measure the electrochemical performance of the synthesized nanomaterials, various percentages of metals such as 10Bi–Fe_2O_3@GO, 20Bi–Fe_2O_3@GO, 30Bi–Fe_2O_3, and GO were evaluated for oxygen evolution reaction (OER). The typical electrochemical measurements were performed in an alkaline condition of 1 M KOH using a workstation (Gamry 600) consisting of three electrodes dipped in the electrochemical cell [15]. LSVs were collected to get information about the onset potential, overpotential, and current density through the polarization curves. The voltammogram pattern demonstrates onset potential, and the current density of catalysts depends on the loading concentration (Fig. 5a). The onset potential for OER is indicated by the area of the voltammogram, where current density was found to increase by

increasing the amount of catalyst. For instance, low onset potential (1.48 V) is observed using 20Bi–Fe_2O_3@GO, which is increased to 1.54 V on increasing the percentages of metal loading to 30Bi–Fe_2O_3@GO and 1.7 V with blank GO sample. Similarly, overpotential values of 250, 370, 520, and 490 mV were observed against 20, 30, and 10Bi-doped Fe_2O_3@GO, and Fe_2O_3@GO respectively, to execute OER whereas, a high overpotential value of 650 mV was attained using pure GO. By looking at the potential of LSV, the small oxidation peak of the metals followed by the exponential increase in the current density indicates the comparative competency of the 20Bi–Fe_2O_3@GO catalyst. However, due to the broadness of the peak, it cannot be attributed to single metals because many factors can affect the potential range of a redox couple. From LSVs, it is evident that the execution potential of OER is changed by changing the Bi concentration in the whole composite materials. CV and stability profile of bare Fe_3O_3 were also collected for comparison. Although the onset potential (1.55 V) was found smaller than 10Bi–Fe_2O_3@GO, however the smaller current density (25 mA/cm^2) and less stability with demand of high potential implies the role of Bi and underlying support (Fig S2). Generally, better OER performance is expected by a high current density at a low overpotential. The current density of 50 mA/cm^2 is attained for an optimized metal-loaded catalyst (20Bi–Fe_2O_3@GO) at a low potential (1.55 V). Hence, the newly synthesized graphene-supported electrocatalysts with optimum loading were found effective for a rapid OER process on the surface of the electrode.

Another measuring parameter that provides information about the kinetics and mechanism of OER is the Tafel slope [22]. It is well understood that the reaction will be faster if the Tafel slope is smaller, and vice versa. Therefore, Tafel Slope values for each synthesized electrocatalyst have been calculated from the LSVs to get information about the kinetics of the reaction. To plot a graph between the log of current density (log j) and overpotential, a certain potential region of LSV data right after onset potential was picked for the Tafel slope shown in Fig. 5b. The slope values of 65, 92, 98, 175, and 200 mV/dec were calculated for 20Bi–Fe_2O_3@GO, 30Bi–Fe_2O_3@GO, 10Bi–Fe_2O_3@GO, F_2O_3@GO, and GO, respectively. To measure the electrochemical performance of the synthesized nanomaterials, various percentages of metals on GO, such as 10Bi–Fe_2O_3@GO, 20Bi–Fe_2O_3@GO, 30Bi–Fe_2O_3@GO were evaluated for oxygen evolution reaction (OER). The favorable kinetic behavior can be observed from the abrupt increase in the current

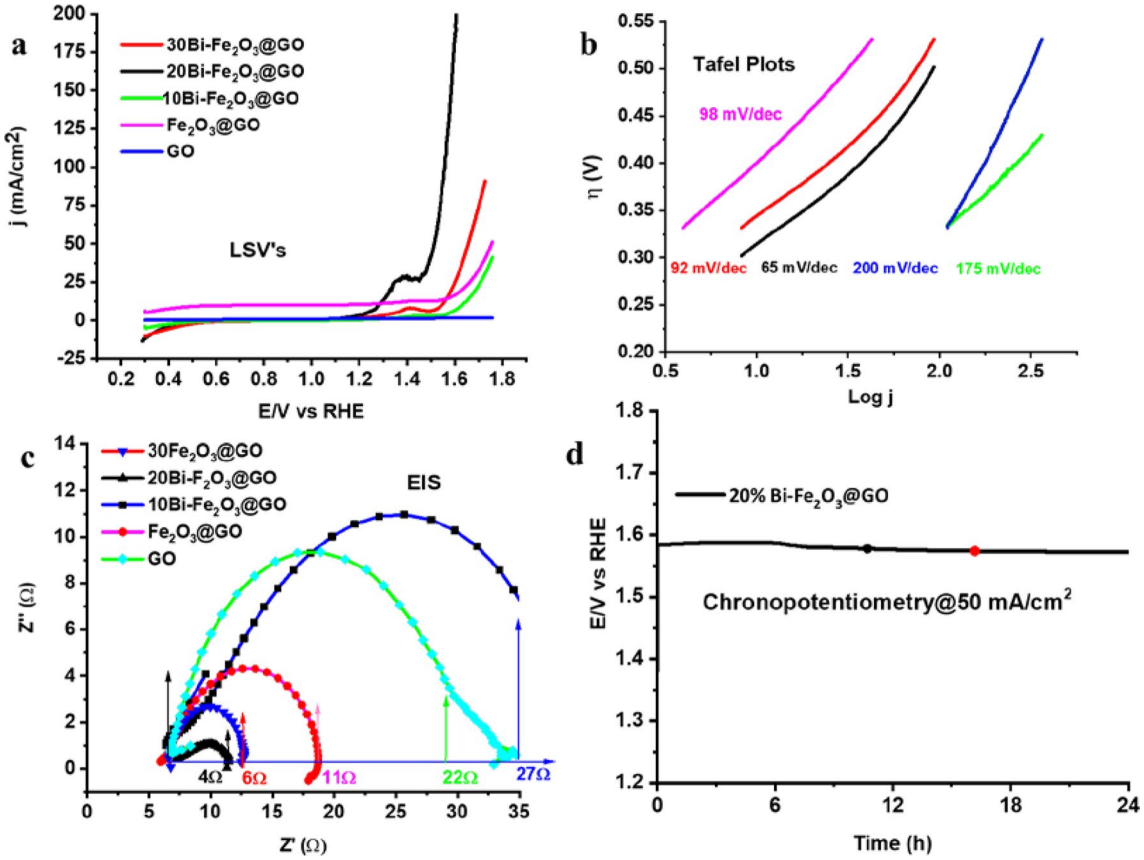

Fig. 5 Electrocatalysis **a** Linear swap voltammogram (LSV) of Bi–Fe_2O_3@GO, Fe_2O_3@GO, and GO in 1 M KOH with a scan rate of 50 mV/s. **b** Corresponding Tafel plots and **c** EIS of the synthesized catalysts **d** Controlled potential electrolysis (CPE) of 20Bi–Fe_2O_3@GO@1.55 V

density with an incremental increase in the potential window for 20Bi–Fe_2O_3@GO. These results indicated that the percent varying of Bi has a significant role in tuning the kinetics of OER in an alkaline medium.

To determine the activity of the synthesized catalyst based on charge transfer at the interface of electrode and electrolyte, electrochemical impedance spectroscopy (EIS) was performed [22]. EIS provides information about intrinsic and charge transfer potential through the charge transfer resistance (Rct). The internal resistance will be lower if the charge transfer is small, which will ultimately enhance the fast electron transfer ability of the catalyst. A Nyquist plot between the real and imaginary parts of the impedance to demonstrate the EIS data collected in alkaline conditions is presented in Fig. 5c. The semicircle from lower to higher frequency with respective values is represented with arrows for convenience. The diameter of semicircles in the Nyquist plot represents the kinetics and charge transfer resistance (Rct), where the lowest value of Rct (4–5 Ω) for 20Bi–Fe_2O_3@GO indicates low internal resistance to subsequently facilitate the electrons transfer during the catalytic process. The small Rct indicates the strong electronic coupling across the whole composite material and can be favorably optimized by changing the composition of the catalyst. Based on the above parameters, we can deduce that the nature of the support, the type of metal, and the quantity of metal loading collectively contribute to the catalytic process. Results of LSVs, Tafel slope, and EIS demonstrated that 20Bi–Fe_2O_3@GO is among the best catalysts for OER (Table S3). Results revealed that the performance of the catalyst is attributed to the optimum doping of Bi and the development of heterointerfaces across the whole hybrid material.

Finally, the stability of the synthesized catalyst was investigated by chronopotentiometry to calculate the current density and electrocatalysis potential. Generally, the activity loss, leaching of the sample, and conversion of catalytic material into inactive form spoils the catalytic activity of catalysts due to harsh conditions during water oxidation [23]. A controlled current electrolysis experiment was performed, where the initial increase and later decrease in the potential is observed to deliver a current density of 50 mA/cm^2 (Fig. 5d). It is noteworthy to mention that due to the broad redox peak and high current density close to the oxidation potential of metals, it may not be technically correct to attribute the stability at low current density to the catalyst. The fluctuation observed in the potential indicated the gradual activation of the active site during catalysis. The long-term (24 h) anodic process rules out the leaching or structural changes in the catalyst which is more easy after comparison with the stability profile of bare Fe_3O_3 (Fig S3). To analyze the catalytic active sites, mass activity, and exchange current density were calculated from the steady state LSV at a particular potential Fig. 6. A gradual increase in the exchange current density and mass activity was observed by increasing the doping of Bi to a certain level which indicates the efficiency of catalyst per unit mass. The observed findings entail that nanostructuring of the materials and optimum doping of hetero-metals on conducting support could provide a plethora of active sites and heterointerfaces, which can increase the chance of collision of different intermediates to enhance the surface catalysis process.

4 Conclusion

Energy conversion and storage are crucial for fostering a sustainable future, wherein alternative and renewable energy sources assume pivotal roles. Recent research has focused on developing bismuth-doped iron oxide on exfoliated graphene oxide nanocomposites, exploring their catalytic potential for the oxygen evolution reaction (OER). We

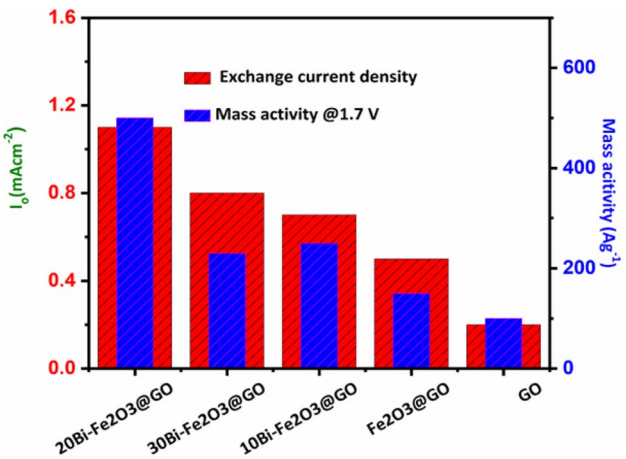

Fig. 6 Graph of exchange current density and mass activity of the synthesized electrocatalysts and GO

have successfully identified the most efficient electrocatalyst through meticulous optimization of metal loading and its distribution across the conducting graphene oxide. Characterization of the prepared nanocomposites of various Bi loading was conducted using Scanning Electron Microscopy (SEM), Transmission Electron Microscopy (TEM), Energy Dispersive X-ray Spectroscopy (EDX), Inductively Coupled Plasma Optical Emission Spectroscopy (ICP-OES and X-ray Diffraction (XRD). Diverse electrochemical parameters such as Linear Swap Voltammetry (LSV), Tafel Slope analysis, stability assessments, Electrochemical Impedance Spectroscopy (EIS), and mass activity measurements were employed to scrutinize the catalytic process. Notably, the electrochemical parameters underscored that an optimized metal loading on the support significantly augments catalytic potential. The 20Bi–Fe_2O_3 composite exhibited compelling characteristics, including low overpotential (250 mV), high current density (200 mA/cm^2@1.6 V), minimal Tafel slope value (65 mV/dec), and low charge transfer resistance (4–5 Ω). These properties are subject to favorable modulation through the manipulation of composition-loading and the nature of the supporting material. Moreover, leveraging their inherent synergistic effects, the integration of bimetallic nanoparticles and their composites emerge as promising and cost-effective catalytic systems.

Acknowledgements We acknowledge Pakistan's Higher Education Commission (HEC) for supporting the research work.

Author contributions Conceptualization, methodology, and draft writing: A.M.; visualization, administration, draft editing, and data verification: H.Y.G; Data processing and analysis: A.H., and M. N.; Data verification and discussion: S.J, M.Z., and J.I, Methodology: A.M., A.H., and A.A. All authors have read and agreed to the published version of the manuscript.

Data availability The reported data in the manuscript will be provided if required.

Declarations

Competing Interest The authors declare no competing interests.

References

1. Leitner W, Quadrelli EA, Schlögl R. Harvesting renewable energy with chemistry. Green Chem. 2017;19(10):2307–8.
2. Lee Y, Suntivich J, May KJ, Perry EE, Shao-Horn Y. Synthesis and activities of rutile IrO2 and RuO2 nanoparticles for oxygen evolution in acid and alkaline solutions. J Phys Chem Lett. 2012;3(3):399–404.
3. Chen FY, Wu ZY, Adler Z, Wang H. Stability challenges of electrocatalytic oxygen evolution reaction: from mechanistic understanding to reactor design. Joule. 2021;5(7):1704–31.
4. Vij V, Sultan S, Harzandi AM, Meena A, Tiwari JN, Lee W-G, Kim KS. Nickel-based electrocatalysts for energy-related applications: oxygen reduction, oxygen evolution, and hydrogen evolution reactions. ACS Catal. 2017;7(10):7196–225.
5. Panapitiya G, Wang H, Chen Y, Hussain E, Jin R, Lewis JP. Structural and catalytic properties of the Au 25–x Ag x (SCH 3) 18 (x= 6, 7, 8) nanocluster. Phys Chem Chem Phys. 2018;20(20):13747–56.
6. Razmjooei F, Singh KP, Yang D-S, Cui W, Jang YH, Yu J-S. Fe-treated heteroatom (S/N/B/P)-doped graphene electrocatalysts for water oxidation. ACS Catal. 2017;7(4):2381–91.
7. Munir A, Haq TU, Qurashi A, Rehman HU, Ul-Hamid A, Hussain I. Ultrasmall Ni/NiO nanoclusters on thiol-functionalized and-exfoliated graphene oxide nanosheets for durable oxygen evolution reaction. ACS Appl Energy Mater. 2018;2(1):363–71.
8. Thomas B, Tang C, Ramírez-Hernández M, Asefa T. Incorporation of bismuth increases the electrocatalytic activity of cobalt borates for oxygen evolution reaction. ChemPlusChem. 2023;88(5):e202300104.
9. Anand P, Jaihindh DP, Chang W-K, Fu Y-P. Tailoring the Ca-doped bismuth ferrite for electrochemical oxygen evolution reaction and photocatalytic activity. Appl Surf Sci. 2021;540:148387.
10. Wu L, Liang Q, Zhao J, Zhu J, Jia H, Zhang W, Cai P, Luo W. A Bi-doped RuO2 catalyst for efficient and durable acidic water oxidation. Chin J Catal. 2023;55:182–90.
11. Liu L, Corma A. Metal catalysts for heterogeneous catalysis: from single atoms to nanoclusters and nanoparticles. Chem Rev. 2018;118(10):4981–5079.

12. Shah LA, Rehman TU, Khan M. Synthesis of graphene oxide doped poly (2-acrylamido-2-methyl propane sulfonic acid)[GO@ p (AMPS)] composite hydrogel with pseudo-plastic thixotropic behavior. Polym Bull. 2020;77(8):3921–35.
13. Marcano DC, Kosynkin DV, Berlin JM, Sinitskii A, Sun Z, Slesarev A, Tour JM. Improved synthesis of graphene oxide. ACS Nano. 2010;4(8):4806–14. https://doi.org/10.1021/nn1006368.
14. Moitra D, Dhole S, Ghosh BK, Chandel M, Jani RK, Patra MK, Ghosh NN. Synthesis and microwave absorption properties of BiFeO3 nanowire-RGO nanocomposite and first-principles calculations for insight into electromagnetic properties and electronic structures. J Phys Chem C. 2017;121(39):21290–304. https://doi.org/10.1021/acs.jpcc.7b02836.
15. Munir A, Qureshi A, Rehman H. Ultrasmall Ni/NiO nanoclusters on thiol functionalized and exfoliated graphene oxide nanosheets for durable oxygen evolution reaction. ACS Appl Energy Mater. 2018;2:1–21.
16. Zhang Q, Yang Y, Fan H, Feng L, Wen G, Qin LC. Synthesis of graphene oxide using boric acid in hummers method. Colloids Surf, A. 2022;652:129802.
17. Kalita H, Palaparthy VS, Baghini MS, Aslam M. Electrochemical synthesis of graphene quantum dots from graphene oxide at room temperature and its soil moisture sensing properties. Carbon. 2020;165:9–17.
18. Long WJ, Gu YC, Xiao BX, Zhang QM, Xing F. Micro-mechanical properties and multi-scaled pore structure of graphene oxide cement paste: synergistic application of nanoindentation, X-ray computed tomography, and SEM-EDS analysis. Constr Build Mater. 2018;179:661–74.
19. Surekha G, Krishnaiah KV, Ravi N, Suvarna RP (2020) FTIR, Raman, and XRD analysis of graphene oxide films prepared by modified Hummers method. In Journal of Physics: Conference Series vol 1495(1), p 012012. IOP Publishing
20. Fominykh K, Feckl JM, Sicklinger J, Döblinger M, Böcklein S, Ziegler J, Bein T. Ultrasmall dispersible crystalline nickel oxide nanoparticles as high-performance catalysts for electrochemical water splitting. Adv Func Mater. 2014;24(21):3123–9.
21. Gong M, Zhou W, Kenney MJ, Kapusta R, Cowley S, Wu Y, Yang J. Blending Cr2O3 into a NiO–Ni electrocatalyst for sustained water splitting. Angew Chem Int Ed. 2015;54(41):11989–93.
22. Chai YM, Zhang XY, Lin JH, Qin JF, Liu ZZ, Xie JY, Dong B. Three-dimensional VOx/NiS/NF nanosheets as efficient electrocatalyst for oxygen evolution reaction. Int J Hydrogen Energy. 2019;44(21):10156–62.
23. Barros KS, Martí-Calatayud MC, Scarazzato T, Bernardes AM, Espinosa DCR, Pérez-Herranz V. Investigation of ion-exchange membranes employing chronopotentiometry: a comprehensive review on this highly informative and multipurpose technique. Adv Coll Interface Sci. 2021;293:102439.